

## Passive vibration controllers with zero dynamic reaction

Abdoulrasoul Sohoul<sup>1</sup>, Zuzana Dimitrovová<sup>2</sup>, Helder C. Rodrigues<sup>3</sup>

<sup>1</sup> IDMEC, Department of Mechanical Engineering, Technical University of Lisbon ([rasoul.sohouli@gmail.com](mailto:rasoul.sohouli@gmail.com))

<sup>2</sup> UNIC, Department of Civil Engineering, Nova University of Lisbon ([zdim@fct.unl.pt](mailto:zdim@fct.unl.pt))

<sup>3</sup> IDMEC, Department of Mechanical Engineering, Technical University of Lisbon ([hcr@ist.utl.pt](mailto:hcr@ist.utl.pt))

### 1. Abstract

Recent progress in material processing and manufacturing have motivated increased interest of the scientific community in material optimization. Tailoring material properties to achieve the optimal response to a given solicitation provides an important input to the new materials development. This paper is focused on material model identification and posterior optimization of its material parameters in order to achieve zero dynamic reaction (zero transmissibility) in passive vibration one-dimensional controllers. Material models that allow for zero dynamic reaction are identified by analytical evaluation of transmissibility. Then parameters characterizing non-linear behaviour of selected components of the chosen material model are optimized by generic probabilistic metaheuristic algorithm simulated annealing. The optimization procedure is programmed within MATLAB environment. It is concluded that optimized designs have no distinguished feature and moreover the corresponding reaction suffer from high reaction peak in the initial transient region. Therefore optimization is extended to the transient region as well. Then plateau at the equilibrium force level is clearly identifiable.

**2. Keywords:** Passive vibration control, material models, optimization, simulated annealing

### 3. Introduction

The theory of non-linear vibration isolation has witnessed significant developments due to pressing demands for the protection of structural installations, mechanical components, and sensitive instruments from earthquake ground motion, shocks, and impact loads. In view of these demands, engineers and physicists have developed different types of nonlinear vibration isolators [1]. Recent studies on quasi-zero stiffness isolators, i.e. isolators that have a plateau at the equilibrium force level in the force-displacement diagram, become the focus of research efforts and industrial interest [2, 3].

The latest developments in computational mechanics lead to integrated methodologies that permit not only the structural design and optimization of the mechanical component but also the tailoring of the material properties and consequently the design of new materials. The aim of this paper is to design a one-dimensional passive vibration controller with zero dynamic reaction. Passive vibration control typically addresses only attenuation of the steady-state regime of the structure dynamic response. However in some industrial applications, namely automotive applications, the transient regime should also be considered. The objective function implemented here accommodates contributions from both regimes.

It is assumed that a mass of a given value is connected through a passive isolator to a fixed support. The mass is excited by a time dependent set of forces. In the first step material models that allow for zero dynamic reaction are identified by analytical evaluation of transmissibility. In the second step non-linear behaviour of the selected material model components is optimized by generic probabilistic metaheuristic algorithm simulated annealing. The design space is composed by non-linear load-displacement curves of each spring contained in the discrete material model, while all dampers are linear viscous. Dynamic stability is assured by non-decreasing load-displacement curves. The optimization procedure is programmed within MATLAB [4] environment. Shooting method [5] is used for steady state response determination.

The results obtained confirm important role of quasi-zero stiffness in passive vibration control. Optimized designs can have a direct and immediate impact on product design and development, especially in the project of new mechanical components such as engine mounts and/or new suspension systems.

### 4. The computational tool

The computational tool, developed in MATLAB environment, is described in details in [6]. It determines macroscopic optimized one-dimensional isolator behaviour assuming that the isolator is represented by a material model with non-linear components. The objective function controls displacement and/or force reaction and has contributions from both regimes; transient and steady state. If excitation is imposed by step force  $P_0$  with harmonic component  $P_1 \sin(\omega t + \varphi)$ , then the value of the objective function related to some admissible isolator behaviour  $S(u, \dot{u})$  is calculated as:

$$O(S(u, \dot{u})) = \gamma_{tr} A_{tr} + \gamma_{st} A_{st} \quad (1)$$

where  $t_r$  is the time separating transient and steady-state regimes and  $t_f$  identifies the final time.  $P_1$  is the amplitude of the harmonic component and  $\omega$ ,  $\varphi$  are the circular frequency and the phase shift. In Eq. (1)  $A_{tr}$  and  $A_{st}$  are the transient and steady-state regime contributions to the objective function weighted respectively by the coefficients  $\gamma_{tr}$  and  $\gamma_{st}$ , satisfying  $\gamma_{tr} + \gamma_{st} = 1$ .  $A_{tr}$  and  $A_{st}$  are given by:

$$A_{tr} = \frac{\alpha_{tr}}{\|R\|} \left( \max_{t \in (0; t_r)} R(t) - \min_{t \in (0; t_r)} R(t) \right) + \frac{1 - \alpha_{tr}}{\|u\|} \left( \max_{t \in (0; t_r)} u(t) - \min_{t \in (0; t_r)} u(t) \right) \quad (2)$$

$$A_{st} = \frac{\alpha_{st}}{\|R\|} \left( \max_{t \in (t_r; t_f)} R(t) - \min_{t \in (t_r; t_f)} R(t) \right) + \frac{1 - \alpha_{st}}{\|u\|} \left( \max_{t \in (t_r; t_f)} u(t) - \min_{t \in (t_r; t_f)} u(t) \right)$$

The weights  $\alpha_{tr}$  and  $\alpha_{st}$  express the relative importance of the reaction versus displacement in each regime and  $\|R\|$ ,  $\|u\|$  are convenient norms related to the particular application. All parameters and weights  $\gamma_{tr}$ ,  $\gamma_{st}$ ,  $\alpha_{tr}$ ,  $\alpha_{st}$ ,  $\|R\|$ ,  $\|u\|$  are user input values and permit the objective function specialization for a large set of practical situations. If a set of  $q$  forces is imposed, then the objective function is given by:

$$O(S) = \sum_{i=1}^q \lambda_i O_i(S) \quad (3)$$

where the respective weights  $\lambda_i$ , satisfying

$$\sum_{i=1}^q \lambda_i = 1 \quad (4)$$

must be defined according to given criteria such as importance of the particular load or probability of occurrence.

Once defined the objective function, the optimization procedure searches for the optimal isolator behaviour  $S^*(u, \dot{u})$ , which solves the optimization problem

$$O(S^*) = \min_{S \in \Xi} O(S) \quad (5)$$

where  $\Xi$  defines the set of admissible isolator behaviours.

The main objective of this paper is to identify and optimize material models that allow for zero dynamic reaction. To accommodate this, only the reaction contribution in the steady-state regime can be considered, *i.e.*  $\gamma_{tr} = 0$  and  $\alpha_{st} = 1$ . Then the objective function value is proportional to the transmissibility  $T$ . In fact if one defines  $\|R\| = 2P_1$  then:

$$O(S(u, \dot{u})) = \frac{1}{2P_1} \left( \max_{t \in \langle t_r, t_f \rangle} R(t) - \min_{t \in \langle t_r, t_f \rangle} R(t) \right) = T \quad (6)$$

## 5. Material model identification

As mentioned before, material models that allow for zero transmissibility can be identified analytically. Transmissibility can be expressed for any material model with linear components in complex range by:

$$T = \left| \frac{R}{P} \right| = \left| \frac{K^*}{K^* - \omega^2 M} \right| \quad (7)$$

where  $R$  is the reaction,  $P$  is the applied harmonic load,  $K^*$  is the complex stiffness and  $\omega$  is the excitation frequency. For instance for Voigt and standard model (Figure 1) the transmissibility according to Eq. (7) is given by:

$$T = \frac{\sqrt{K^2 + C^2 \omega^2}}{\sqrt{(K - \omega^2 M)^2 + C^2 \omega^2}} \quad \text{and} \quad T = K_1 \sqrt{\frac{K_2^2 + C^2 \omega^2}{(K_1 K_2 - \omega^2 M (K_1 + K_2))^2 + C^2 \omega^2 (K_1 - \omega^2 M)^2}} \quad (8)$$

respectively.

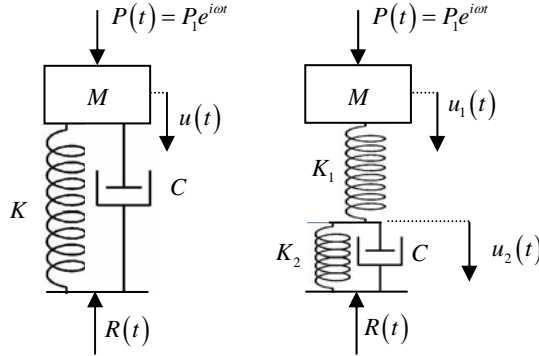


Figure 1. Voigt and standard model

For non-negative spring rigidities this means that the minimum values for the above named models are

$$T = \frac{C}{\sqrt{(M\omega)^2 + C^2}} \quad \text{and} \quad T = 0 \quad (9)$$

In conclusion, and as shown in [6], zero transmissibility is unachievable by Voigt model, but there are several material models that permit such an extreme value, like for instance the standard model. By analysis of Eq. (9) it is readily seen that in Voigt model this minimum value is increasing with the increasing damping coefficient. Regarding the standard model, from Eq. (9) it is seen that the rigidity  $K_1$  is decisive for achieving the zero transmissibility.

## 6. The set of admissible isolator behaviours

For any material model it is assumed that dampers are linear viscous characterized by damping coefficients and that springs have non-linear behaviour. The non-linear behaviour is specified by load-displacement curves. According to practical applications, there is an initial and a final linear stage characterized by the initial  $K_{ini}$  and final  $\bar{K}_{fin}$  rigidity. Admissible designs follow the initial rigidity,

have the final rigidity  $K_{fin}$  that is higher or equal to  $\bar{K}_{fin}$  and within the design window, specified by  $[0, u_{ma}] \times [0, F_{ma}]$ , can possess any behaviour that is characterized by continues increasing curve. For numerical reasons the admissible designs are specified by piece-wise monotonic Hermitian polynomials, because continuous derivatives of the load-displacement curve are a necessary condition for the shooting method. Two admissible nonlinear spring designs are illustrated in Figure 2. The variable (dashed and dash-dotted) part of the load-displacement curve is the focus of optimization. The dotted line identifies the “reference” load-displacement curve, piecewise linear defined by slope values  $K_{ini}$ ,  $K_{ref}$  and  $K_{fin} = \bar{K}_{fin}$ , that will be used further on for evaluation of the effectiveness of the optimal solutions. Please note that the reference design does not have continuous derivatives, therefore the shooting method cannot be used and the steady-state response is obtained by the method of “long simulation”.

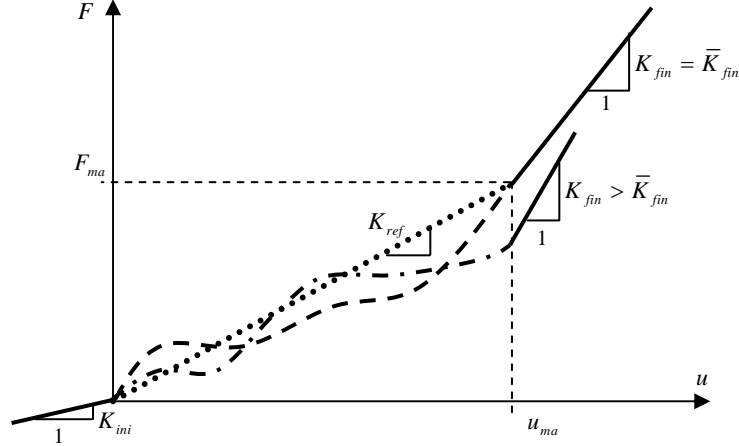


Figure 2. Load-displacement curve for three possible non-linear spring designs. Fixed parts (solid) and variable/designable parts (dashed, dash-dotted, dotted)

It is moreover assumed that the spring behaviour is perfectly hyperelastic, i.e. loading and unloading paths match exactly. For more details consult [6]. To analyze the optimal solution efficiency, a comparison with the value obtained for the “reference design” (defined in Figure 2 by the dotted line) is performed. Efficiency  $E$  is expressed as:

$$E = \frac{O_{ref} - O_{opt}}{O_{ref}} \quad (10)$$

where  $O_{opt}$  is the optimal design objective function value and  $O_{ref}$  is the value obtained for the reference design.

## 7. Numerical examples

As specified before, the main objective is to obtain zero dynamic reaction, therefore only the reaction contribution in the steady-state regime is considered. For the sake of simplicity  $\|R\|=1$ . The standard material model according to Figure 1 is chosen, because this model allows for the zero dynamic reaction as shown in Eq. (9).

Design space is defined according to practical applications [7] as:  $u_{ma} = 10\text{mm}$ ,  $F_{ma} = 1500\text{N}$ ,  $\bar{K}_{fin} = 1\text{MN/m}$ , thus giving  $K_{ref} = 150\text{kN/m}$  (see Figure 2). It is moreover assumed that the mass of the object to be isolated is  $M = 50\text{kg}$  and that the displacement is measured from the equilibrium position, when the isolator is loaded by the object weight. The damping coefficient in [6] was varied between 100, 200 and 400  $\text{N} \cdot \text{s/m}$ . It was shown that in Voigt model high damping is less efficient in the steady-state regime (compare with Eq. (9)). For this reason here only  $C = 400\text{N} \cdot \text{s/m}$  is considered.

### 7.1 Case study 1

The Case study 1 corresponds to application of single step force with harmonic component  $P = 400 + 200\sin(300t)[\text{N}]$ . The objective is to identify non-linear force-displacement curves for the two springs of the standard material model in order to achieve zero transmissibility. The optimized design is shown in Figure 3 and the objective function values for optimized and reference designs are summarized in Table 1.

Table 1. The optimization analysis for the Case study 1

$\gamma_{tr}$	$O_{opt}$ (N)	$O_{anal}$ (N)	$O_{ref}$ (N)	$E$ (%)
0	0.0054	0.0000	8.8091	99.94%

As shown analytically, Spring 1 should have a plateau at the equilibrium force level within the steady state displacement range, but for zero transmissibility, the steady-state range “does not exist”, therefore the plateau is not visible. Plateau in Spring 2 is not necessary. Steady-state displacement and reaction is shown in Figures 4 and 5. The phase plane is shown in Figure 6. In Figure 7 the reaction in the optimized design is compared with the reaction in the reference design, but now with the inclusion of the transient part, admitting the homogeneous initial conditions. It is seen that under these conditions the reaction in the optimized design does not show any improvement. Therefore the optimization search was extended to the transient range as well and several values of  $\gamma_{tr}$  were tested. Results are summarized in Table 2. It is seen that then the objective function is higher, but this is mainly because of the

transient contribution. Nevertheless, it is necessary to point out that for initial conditions matching the existence of the periodic solution, such a reaction peak would be removed.

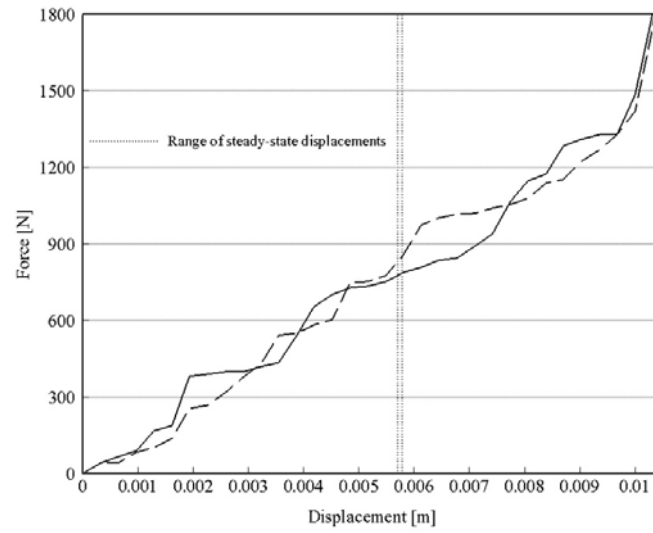


Figure 3. Optimized design of the load-displacement curves in the Case study 1,  $\gamma_{tr} = 0$  (Spring 1: solid curve, Spring 2: dashed curve)

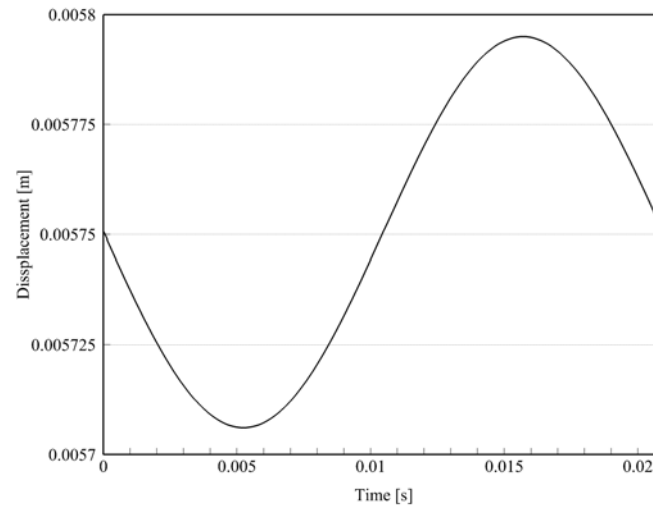


Figure 4. Steady-state displacement of the isolated object in the Case study 1,  $\gamma_{tr} = 0$

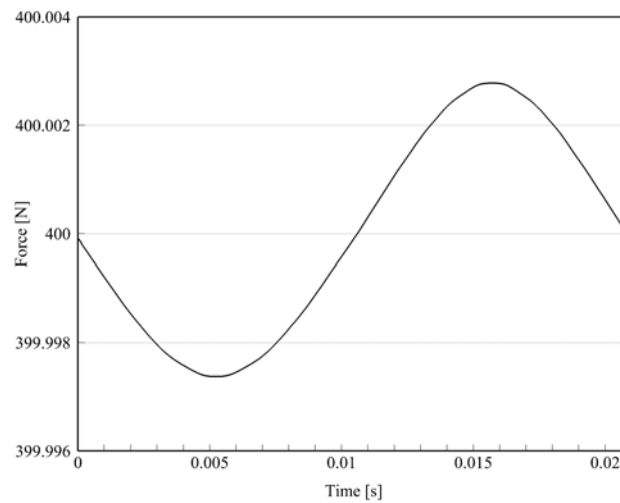


Figure 5. Steady-state reaction in the Case study 1,  $\gamma_{tr} = 0$

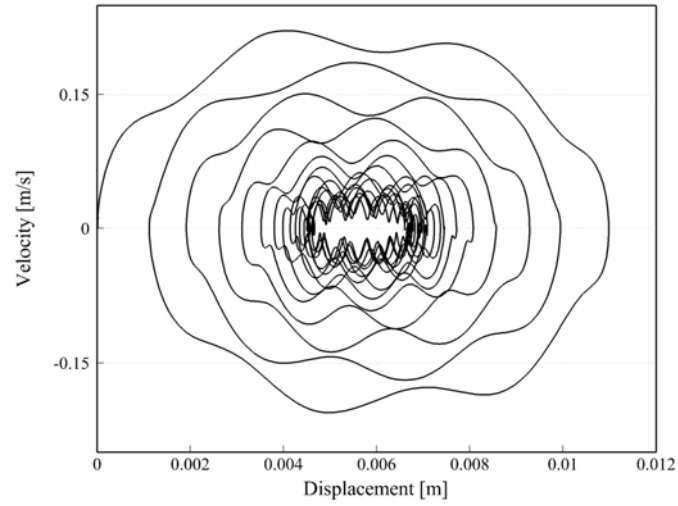


Figure 6. Phase plane in the Case study 1,  $\gamma_{tr} = 0$

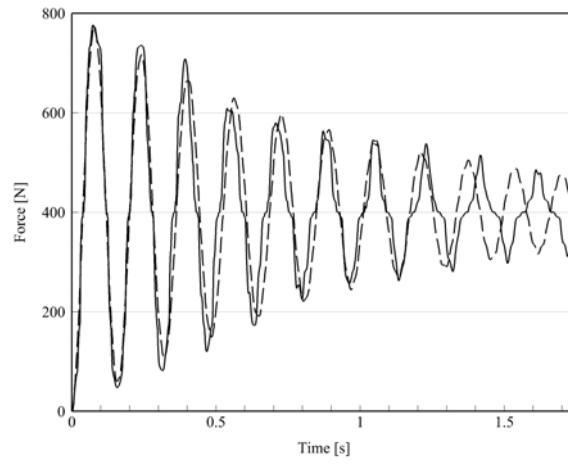


Figure 7. Reaction including the transient part in the Case study 1,  $\gamma_{tr} = 0$ , under homogeneous initial conditions (Optimized: solid curve, Reference: dashed curve)

Reaction comparison is shown in Figure 8 under homogeneous initial conditions. It is seen that the initial reaction peak is significantly reduced. It is also seen that there is an initial “amplitude” affecting the objective function value, but this part is rapidly attenuated. Optimized designs have now clearly defined plateau in Spring 2 (Figures 9-10).

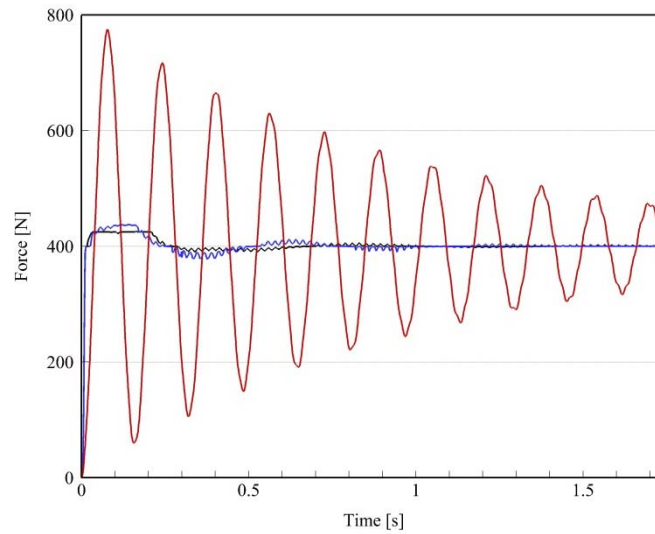


Figure 8. Reaction force comparison ( $\gamma_{tr} = 0.01$  : Blue curve,  $\gamma_{tr} = 0.25$  : Black curve and Reference design: Red curve)

Table 2. Summary of the optimization analysis for the Case study 1 regarding various  $\gamma_{tr}$

$\gamma_{tr}$	$O_{opt}$ (N)
0.25	9.1488
0.02	0.8215
0.01	0.5793

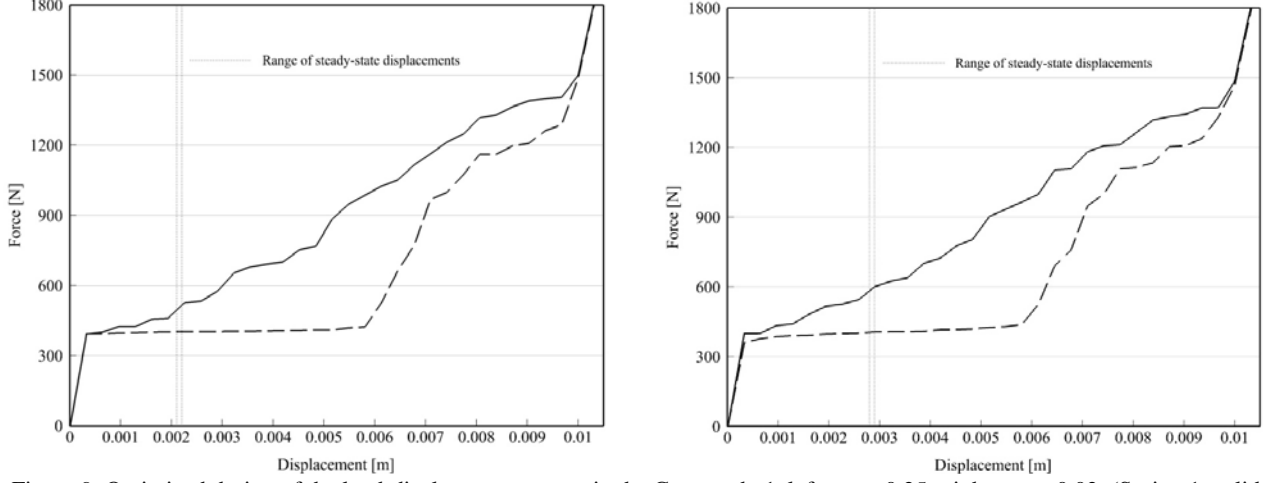


Figure 9. Optimized design of the load-displacement curves in the Case study 1, left:  $\gamma_{tr} = 0.25$  , right:  $\gamma_{tr} = 0.02$  (Spring 1: solid curve, Spring 2: dashed curve)

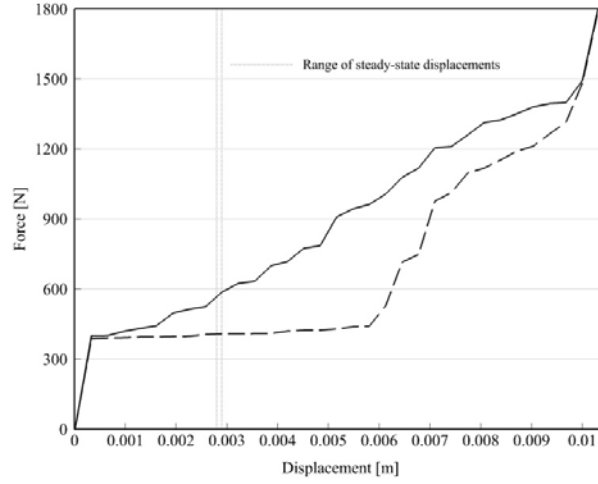


Figure 10. Optimized design of the load-displacement curves in the Case study 1,  $\gamma_{tr} = 0.01$  (Spring 1: solid curve, Spring 2: dashed curve)

## 7.2 Case study 2

In the previous section optimization to one specific load was shown. This is rarely a case of practical interest. Therefore in this section the case study involving four loads with the same probability of occurrence 0.25 is considered. Four step forces with superimposed harmonic components are considered: namely the step loads  $P_{0,1} = 300\text{N}$  ,  $P_{0,2} = 400\text{N}$  ,  $P_{0,3} = 500\text{N}$  ,  $P_{0,4} = 600\text{N}$  and the respective harmonic forces amplitudes  $P_{1,1} = 300\text{N}$  ,  $P_{1,2} = 250\text{N}$  ,  $P_{1,3} = 200\text{N}$  and circular frequencies:  $\omega_1 = 1200\text{rad/s}$  ,  $\omega_2 = 900\text{rad/s}$  ,  $\omega_3 = 600\text{rad/s}$  ,  $\omega_4 = 300\text{rad/s}$  which yield the common period of 0,021s.

Table 3. The optimization analysis for the Case study 2

$\gamma_{tr}$	Step	$O_{opt}$ (N)	$O_{anal}$ (N)	$O_{ref}$ (N)	$E$ (%)
0	$O$	0.0887	0.0000	3.2486	97.2693
	$\lambda_1 O_1$	0.0207	0.0000	0.2771	92.5297
	$\lambda_2 O_2$	0.0401	0.0000	0.6304	93.6389
	$\lambda_3 O_3$	0.0086	0.0000	0.6492	98.6753
	$\lambda_4 O_4$	0.0193	0.0000	1.6919	98.8593

The phase angle is considered zero in all cases. Results for the case of  $\gamma_r = 0$  are summarized in Table 3.

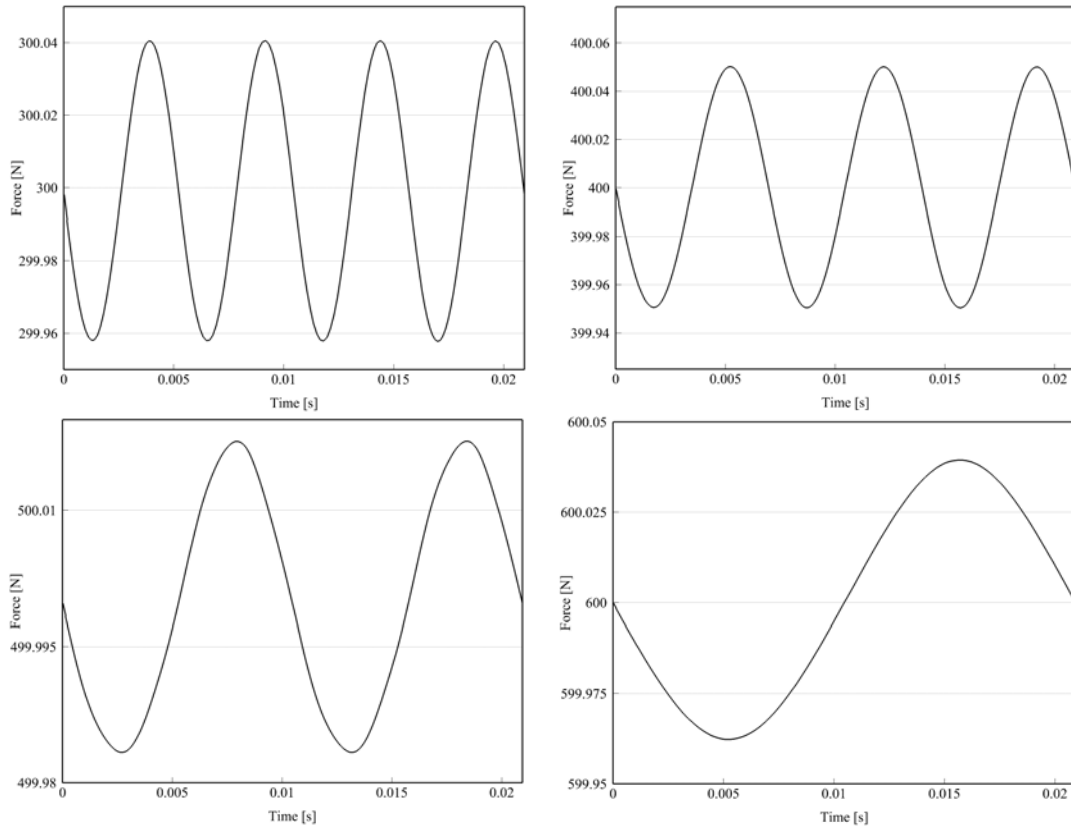


Figure 11. Steady-state reaction of the four forces in the Case study 2,  $\gamma_r = 0$

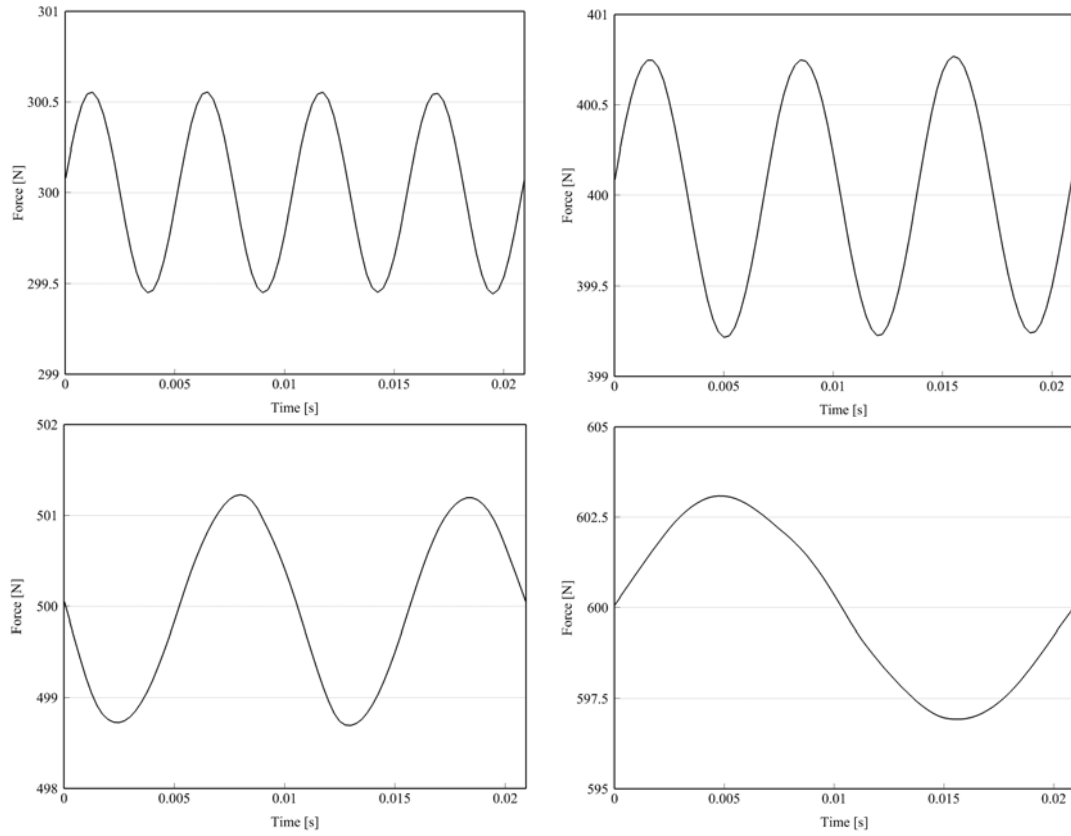


Figure 12. Steady-state reaction of the four forces in the Case study 2 for the reference design

Figures 11 and 12 compare the steady-state reaction of the four forces in the optimized and the reference design. Optimized design is shown in Figure 13.

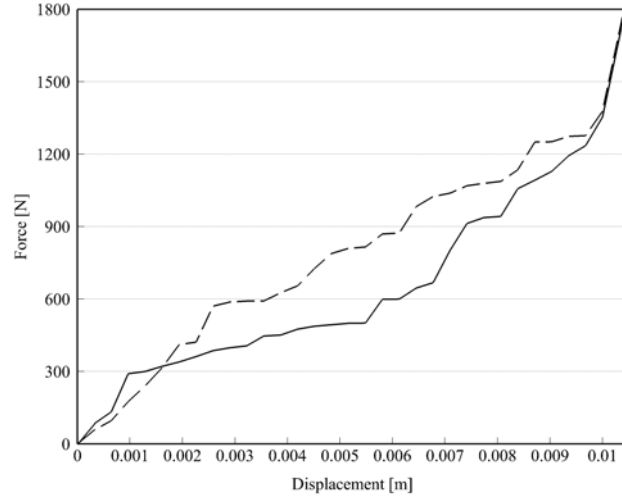


Figure 13. Optimized design of the load-displacement curves in the Case study 2,  $\gamma_{tr} = 0$  (Spring 1: solid curve, Spring 2: dashed curve)

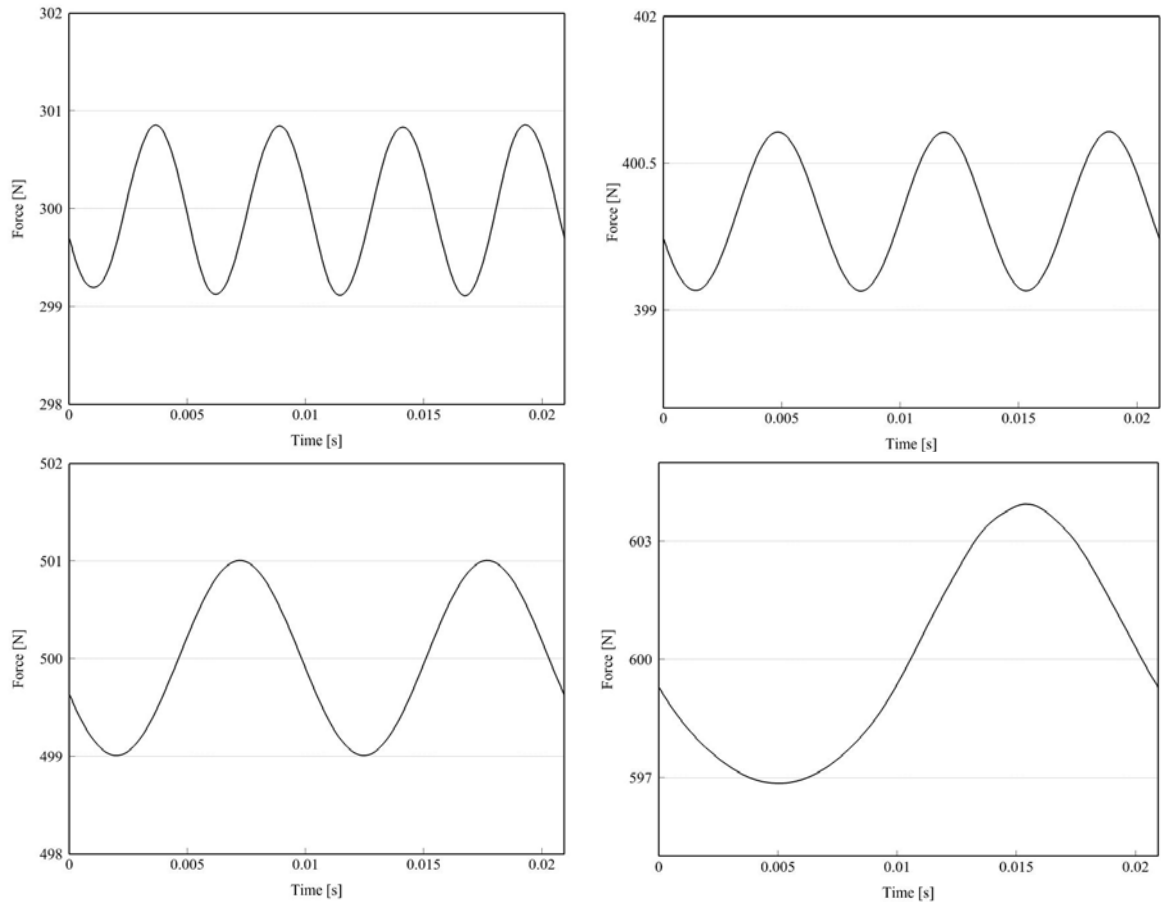


Figure 14. Steady-state reaction of the four forces in the Case study 2,  $\gamma_{tr} = 0.25$

As in the previous section also the influence of  $\gamma_{tr}$  was analyzed. Results are summarized in Table 4. It is seen that the objective function value is higher, but as before, this is caused by the transient contribution. Steady-state parts are shown in Figure 14, where the case of  $\gamma_{tr} = 0.25$  is plotted.



Table 4. Summary of the optimization analysis for the Case study 1 regarding various  $\gamma_{tr}$ 

$\gamma_{tr}$	Step	$O_{opt}$ (N)	$\gamma_{tr}$	Step	$O_{opt}$ (N)
0.01	$O$	9.669	0.25	$O$	151.098
	$\lambda_1 O_1$	2.5960		$\lambda_1 O_1$	22.2911
	$\lambda_2 O_2$	1.5864		$\lambda_2 O_2$	27.1009
	$\lambda_3 O_3$	1.8091		$\lambda_3 O_3$	41.9467
	$\lambda_4 O_4$	3.6893		$\lambda_4 O_4$	59.7591

## 8. Conclusions

The model described in this work, even though one dimensional, captures well the mechanical problem and the main issues that should be tackled in passive vibration control. From the results obtained it is apparent that optimal behaviour can be achieved, however it is also evident that the optimal solution is highly dependent on the problem data, namely applied forces and constraints. Thus a precise definition of existing forces and design constraints is crucial for its success in practical applications.

The results obtained are also dependent on other parameters entering the objective function definition, like several weighting parameters and norms. Therefore the further research will be directed to implementation of multi-objective algorithm.

The drawback of this approach is that there are no clear features of optimized designs that could be generalized and extrapolated to other situations.

## 9. References

1. Balandin D V, Bolotnik N N, Pilkey W D. Optimal Protection from Impact, Shock and Vibration. Gordon and Breach Science, 2001.
2. Platus D L, Smoothing out Bad Vibes, Mach Des, 1993, 26, 123–130.
3. Kovacic I, Brennan M J, Waters T P, A Study of a Nonlinear Vibration Isolator with a Quasi-Zero Stiffness Characteristic, J Sound Vib, 2008, 315, 700–711.
4. Release R2009a Documentation for MATLAB (2009) The MathWorks, Inc.
5. Jirásek M, Simple Non-linear System Simulation. Internal Report, Czech Technical University in Prague, 1988, (in Czech)
6. Dimitrovová Z, Rodrigues H C, Optimization of Passive Vibration Isolators Mechanical Characteristics, Struct Multidiscip O, 2010, 42 (3), 325-340.
7. Zavala P G, Pinto M G, Pavanello R, Vaqueiro J, Experimental and Computational Simulation Approaches for Engine Mounting Development and Certification, SAE Technical Paper Series, 2000, 2000-01-3239E.